Author Queries

JOB NUMBER: MS 176597—
JOURNAL: GNER

Q1 Kindly provide page range and volume for the Reference [13].

GNER 176597—7/5/2006——211820

Journal of Neutron Research, Vol. 14, No. 2, 2006, 1–15

Monte Carlo simulations of a powder diffractometer installed on a long pulse target station using wavelength frame multiplication

K. LIEUTENANT†‡* and F. MEZEI†§

†Hahn-Meitner-Institut Berlin, Glienicker Street 100, D-14109 Berlin, Germany
‡Institut Laue-Langevin, 6 rue Jules Horowitz, F-38042 Grenoble, France
§LANSCE, Los Alamos National Laboratory, Los Alamos, NM 87545, USA

MC simulations of a neutron diffractometer have been performed using the VITESS software package to check the feasibility of the frame multiplication concept and to compare a powder instrument installed on a long pulse target station (LPTS) with an equivalent instrument installed on a decoupled poisoned moderator of a short pulse target station (SPTS) of the same power. The simulations show that frame multiplication can be realised, if five choppers are used to determine the frame. For the same FWHM peak width, the LPTS yields comparable peak intensities for wavelengths of about 1 Å, much higher intensities than the SPTS for long wavelengths, and a quite symmetric peak shape for all wavelengths. Therefore, a combination of high-energy LPTS and pulse shaping choppers can be used instead of a decoupled poisoned moderator of a SPTS to run a TOF powder diffractometer. It is the better choice (than the SPTS solution), because it matches the performance of SPTS in the case most favourable for SPTS: highest resolution offered by the poisoned moderator, has the capability of easily increasing the intensity by its variable resolution and gives superior intensity for longer neutron wavelengths.

Keywords: MC simulations; Pulsed neutron source; Diffractometer; Frame multiplication; Beam extraction system; Ballistic guide

1. Introduction

Diffractometers installed on pulsed neutron sources need short pulses to achieve a good resolution. Therefore, diffractometers are usually installed on short pulse target stations (SPTS) normally using a decoupled moderator. Alternatively, such an instrument can be installed on a long pulse target station (LPTS), if pulse-shaping choppers are used that cut a short pulse out of the long pulse. It was already shown that such a system can be advantageous compared to the installation on a SPTS [1].

The basic idea is to put a fast rotating chopper (disc chopper or Fermi chopper) as close as possible to the source and to project the pulse to the detector like in a pin-hole camera. But due to the shielding, a chopper cannot be positioned as close as desired to the source, for ESS the minimal distance is about 6 m (depending on the beam line) [2]. This restricts the bandwidth of the pulse (cf. equation (2)). Therefore it is possible that the bandwidth that can be delivered by the pulse generation system is smaller than that corresponding to the pulse repetition rate, especially if the repetition rate of the source is low (cf. equations (2) and (3)).

*Corresponding author. Tel.: +33 4 76 20 78 03. Fax: +33 4 76 20 76 48. Email: lieutena@ill.fr

Journal of Neutron Research
ISSN 1023-8166 print/ISSN 1477-2655 online © 2006 Taylor & Francis
http://www.tandf.co.uk/journals
DOI: 10.1080/10238160600766401

To overcome this problem, the concept of "wavelength frame multiplication" was introduced [3]. Here two, three or more frames are used at the same time, i.e. the effective bandwidth of the source (plus pulse shaping choppers) is multiplied by the number of frames used simultaneously. This requires a complicated chopper system.

It is generally believed that a powder diffractometer designed for measuring magnetic structures is especially suited to be run at a SPTS (instead of a LPTS). On the other hand, a diffractometer at LPTS would be more flexible. It is capable of easily increasing the intensity by a factor up to 3–4, by its variable resolution (just by changing the phasing of the first chopper pair). The current considerations remain valid as long as the pulse width remains $<<1$ ms (for the LPTS machine). Thus, it is a special challenge to achieve as good results on a long pulse source as can be obtained on a short pulse source. Therefore, we have chosen this instrument as an example to test the performance on a LPTS. As sources we have used the two target stations proposed for the ESS: 5 MW LPTS (16.667 HZ) and 5 MW SPTS (50 Hz).

Preliminary results of this comparison were already published [4]. Here we present a more detailed description of the instrument with an improved design.

2. Instrument layouts

2.1 Short pulse target station (SPTS)

As instrument on the SPTS, we have simulated the instrument MAGPOW proposed for the ESS [5]. The only difference is that we have installed it on a decoupled poisoned cold moderator instead of a decoupled un-poisoned cold moderator as proposed in Ref. [5], because we wanted to study high-resolution instruments (for an un-poisoned moderator the LPTS machine would have the easy advantage of being able to achieve better resolution if needed and without any loss for the lower resolution mode of operation by its inherent variable resolution capability).

The length of the primary flight path is 50 m. Chopper positions and apertures are simulated as proposed. The guide cross-section is reduced in a 12.5 m long funnel from $80 \times 20\,\text{mm}^2$ (H × W) to $26 \times 13\,\text{mm}^2$ as proposed. Of the different focussing options, we have only simulated the "unfocussed" option assuming a straight guide of 1.5 m length and $26 \times 13\,\text{mm}^2$ cross section with $m = 2$ supermirror coating and 1.0 m free flight path to the sample. (This is not described in detail in Ref. [5]).

Assuming that the design of this instrument was optimised by the authors we did not really try to improve it. But we checked if a coating of $m = 2$ on left and right sides of the straight parts of the guide would improve the design, as a relatively small compression in horizontal direction is used. And we tried to estimate the influence of a ballistic guide [8] by testing an expansion to $40 \times 100\,\text{mm}^2$. The result of the $m = 2$ simulation was that the flux at sample is increased by about 9% for the short wavelength range, while no significant effect was found for the other ranges. The ballistic guide enhanced the flux at sample by about 4% in all ranges (compared to the original instrument).

We used a Ni sample as an example for a small elementary cell and a sample with a large lattice spacing, which is typical for high-T_C superconductors. For the sake of simplicity, a constant sample-detector distance of 2 m was assumed giving a total instrument length of 52 m. Further data are listed in table 1.

2.2 Long pulse target station (LPTS)

The layout of this instrument combines several new approaches for instrument design (cf. [6]): multi-spectral beam extraction [6,7], wavelength frame multiplication [3] and

Table 1. Data of the simulation of the diffractometer at the SPTS.

	Pos. (of beg.) of component (m)	*Rot. freq. of chopper (rpm)*	*Chopper aperture (deg)*	*(guide) Width (cm)*	*(guide) Height (cm)*	*Coating (m) (all surfaces)*
Source	0.00			21.00	12.00	
Guide	1.50			2.00	8.00	1.15
Frame overlap chopper	6.50	3000	42.0			
Frame overlap chopper	10.00	3000	69.0			
Frame definition chp.	12.00	3000	85.0			
Funnel 1 (= end of straight guide)	35.00			2.00	8.00	2.0
Funnel 2	47.50			1.30	2.60	2.0
Free flight path	49.00			1.30	2.60	
Sample	50.00			1.00	2.00	
Detector	52.00			606.00	20.00	

a ballistic guide [8] and uses a special arrangement of the disk choppers to generate pulses which are proportional in length to the wavelength [9]. Choppers are necessary to prevent frame overlap between subsequent pulses and between the frames that are observed at the same time.

2.3 General layout

The equivalent instrument at LPTS needs three times the total length of the instrument at the short pulse source to use the same wavelength band width, because the repetition rate of the pulses is only a third of the rate of the short pulses (with the repetition rates of 50 Hz and (1/3) × 50 Hz planned for the ESS). Therefore the total flight path downstream of the pulse shaping choppers is set to 156 m. The pulse is assumed to be created in the centre of the double chopper system; this is the reference position for all distances mentioned here.

A chopper with an aperture of 180° positioned about half way between source and detector is used as frame definition chopper. A second chopper is positioned 3.44 m after the pulse shaping choppers. It shall prevent overlap between the subsequent long pulses. Both rotate with the frequency of the long pulse source. (The other choppers are discussed in the following sections.)

The last part of the instrument (from 139 to 156 m, cf. figure 1) is identical with the instrument at SPTS (see above).

2.4 Source and extraction system

As source we have used a bi-spectral moderator, H_2 and H_20 coupled moderators side by side (as proposed for the ESS), each 100 mm wide and 120 mm high with 10 mm gap in between. The power of the LPTS is 5 MW as planned for the ESS; but in contrast to the ESS reference [10], the so-called "high energy option" with a pulse length of 1 ms (instead of 2 ms) is assumed. Additionally, an increased intensity of the coupled H_2 moderator (by a factor of 1.5) due to an optimisation of the moderator thickness is presumed, which was achieved after the release of the moderator characteristics. In this way, the flux averaged over 1 ms (see below) was improved by a factor of about 1.6 for the short wavelength band and about 2.4 for the others compared to the reference data [10].

To serve the guide with neutrons of both moderators, a beam extraction system is used [7]. The guide points directly to the thermal source (close to its centre). Three vertical

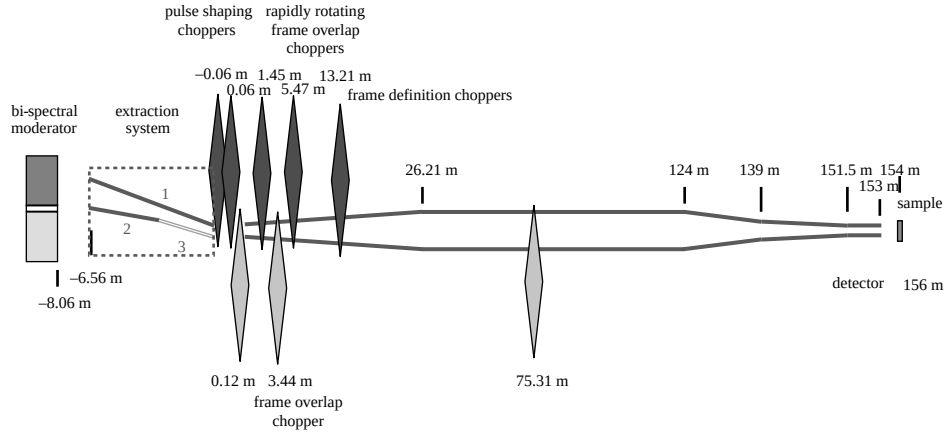

Figure 1. Layout of the powder diffractometer installed on LPTS seen from the top (except for the choppers, which are located below the guide in the simulation). All lengths give the distance from the point of pulse generation supposed to be in the centre of the double disc chopper (positive values = downstream). The moderator consists of a compartment for cold neutrons (dark grey) and one for thermal neutrons (light grey). Mirror 3 of the extraction system is transparent, the two others have a reflecting coating ($m = 3$) on the inner side and an absorbing coating on the outer side. Choppers drawn in light grey rotate with the frequency of the source, the others have a by a factor n higher frequency ($n = 20$, 17, 12 and $7^{2/3}$).

supermirrors ($m = 3$) beginning 1.5 m from the moderator conduct neutrons from the cold source (dark grey) into the guide (figure 1). The mirror in front of the thermal source (mirror 3 in figure 1) is a 0.5 mm thin silicon plate coated with a $m = 3$ supermirror. This mirror allows short wavelength neutrons coming from the thermal moderator (light grey) to pass and to enter the neutron guide, while long wavelength neutrons are reflected. On the other hand, long wavelength neutrons coming from the cold moderator are reflected by this mirror and thus conducted into the neutron guide, while short wavelength neutrons pass through this mirror (if not absorbed before).

The inclination of mirror three defines the wavelength of switch-over between thermal and cold neutrons; a inclination of 0.72° was calculated to be optimal. Because of the thin plate, only a small fraction of the thermal neutrons is absorbed before entering the guide. The absorption inside the silicon has been taken into account.

In order to conduct as many neutrons as possible from the cold source (dark grey) into the guide, a large entrance width of the extraction system is necessary. Also, a small width at the end of the extraction system is required to create short pulses. On the other hand, the inclination of mirror one increases the divergence of the cold neutrons and should therefore not be too large. As a first approximation, apertures of $48 \times 80\,\mathrm{mm}^2$ at the beginning and $15 \times 80\,\mathrm{mm}^2$ at the end of the extraction system have been assumed. In the course of the simulation, the sizes of the extraction system have than be varied to find an optimal set-up (see below).

In addition to the three vertical mirrors, two parallel horizontal mirrors ($m = 3$, $0.19 \times 5.00\,\mathrm{m}^2$, distance 120 mm) covering the vertical mirrors on top and bottom are used for the extraction system. Position and size are indicated by dotted lines in figure 1. (The size can of course be reduced, but a rectangular shape was easiest to use in a simulation). They were introduced to increase the flux from both moderators (which worked because the moderator height is smaller than the acceptance height for wavelengths above 1.18 Å). Further data are listed in table 2.

Table 2. Data of the simulation of the diffractometer at the high-energy LPTS.

	Pos. (of beg.) of component (m)	*Rot. freq. of chopper (rpm)*	*Chopper aperture (deg)*	*(guide) Width (cm)*	*(guide) Height (cm)*	*Coating m (left–right–top/bottom)*
Source	−8.06			21.00	12.00	
Extraction system	−6.56			4.80	8.00	3–3–3
Aperture	−0.06			1.50	8.00	
Pulse shaping chp. 1	−0.06	20000	20.0			
Pulse shaping chp. 2	0.06	20000	20.0			
Pulse select. chopper	0.12	1000	18.0			
Div. part of ball. guide	0.12			1.50	8.00	3–3.5–2
Frame overlap chopper	1.45	17000	43.2	1.65	8.25	3–3.5–2
Frame overlap chopper	3.44	1000	25.0	1.88	8.64	3–3.5–2
Frame overlap chopper	5.47	12000	67.2	2.12	9.03	3–3–2
Sub-frame definit. chp.	3.21	7667	77.9	3.01	10.51	2–2–2
Straight guide	26.21			4.50	13.00	1–1–1
Frame definition chp.	75.31	1000	180.0			
Converging guide	124.00			4.50	13.00	2–2–2
Funnel 1(= end of ballistic guide)	139.00			2.00	8.00	2–2–2
Funnel 2	151.50			1.30	2.60	2–2–2
Free flight path	153.00			1.30	2.60	
Sample	154.00			1.00	2.00	
Detector	156.00			606.00	20.00	

2.5 Pulse generation

The resolution is determined by the ratio of pulse length to instrument length. As the flight path of the LPTS-instrument has three times the length of the SPTS instrument, the pulse length also has to be about three times longer to get the same resolution. The pulse length of the SPTS is roughly proportional to wavelength up to 5.3 Å and has a constant value of *ca* 57 μs for longer wavelengths (see [10]).

To achieve an equivalent wavelength dependence for the LPTS, a pair of choppers rotating in the same sense with a fixed phase shift can be used (chopper 1 is closest to the source, chopper 2 is positioned downstream). If chopper 2 opens when chopper 1 closes, the pulse length is proportional to the time t_c the neutrons need to cross the distance L_c between the choppers

$$t_c \approx \frac{L_c}{V_n} = \frac{L_c m_n}{h\lambda} \tag{1}$$

In Ref. [9]—provided (a) the chopper window is large enough not to cut the pulse and (b) the time t_{cross} the chopper needs to cross the beam is small compared to the t_c ($t_{cross} = 24$ μs, $t_c \geq 45$ μs—table 3). This chopper arrangement yields a constant resolution in wavelength.

Preliminary studies showed that this can be realised by two choppers separated by 12 cm and chopper apertures of 20°. To obtain a constant pulse length for wavelengths above 5.3 Å, the chopper phases must be adapted, i.e. chopper 1 closes before chopper 2 opens. The resulting FWHM widths are listed in table 3.

For the wavelength frame multiplication, the time between two openings of the choppers has to be the pulse length, i.e. about 1 ms (cf. figure 2, next chapter). As the choppers need 3 ms for a rotation (with a planned rotational speed of 20,000 rpm), discs with three apertures have to be used.

This set-up now generates pulses every ms. As only 3 of the 60 frames created per cycle shall be used, all pulses that are not needed have to be cut. This is done by a third chopper running with the frequency of the neutron source, placed 6 cm downstream of the second pulse shaping chopper (three fast choppers in the same housing can be as close as 2–3 cm from each other, example: IN500 in Los Alamos; so 12 and 6 cm distances are state of the art). An opening time of more than 2 ms and less than 4 ms is necessary to let exactly three pulses pass. We used an aperture of 18°, which corresponds to 3 ms.

The first chopper is phased in a way that neutrons of the average desired wavelength coming from the centre of the pulse pass the centre of the chopper. In case of an average wavelength of 4 Å, the three pulses to be used are generated about 6.4, 7.4 and 8.4 ms after the beginning of the pulse. This is seen as the new source for the rest of the chopper system, i.e. the short pulse is ($t_0 = 6.4$ ms,...) delayed compared to the original pulse.

2.6 Wavelength frame multiplication

The short pulses (used for the measurements) are generated by rapidly rotating disc choppers. If the same distance between moderator and first chopper is used as in the instrument on

Table 3. FWHM pulse lengths of both sources for different wavelengths.

Wavelength (Å)	*SPTS*[†]*(μs)*	*LPTS*[‡]*(μs)*
1.5	13	45
4.0	47	122
16.8	57	160

[†] Values extracted from the last picture of the ESS moderator characteristics [10].
[‡] Widths determined in these MC simulations by means of a time monitor positioned after chopper 2.

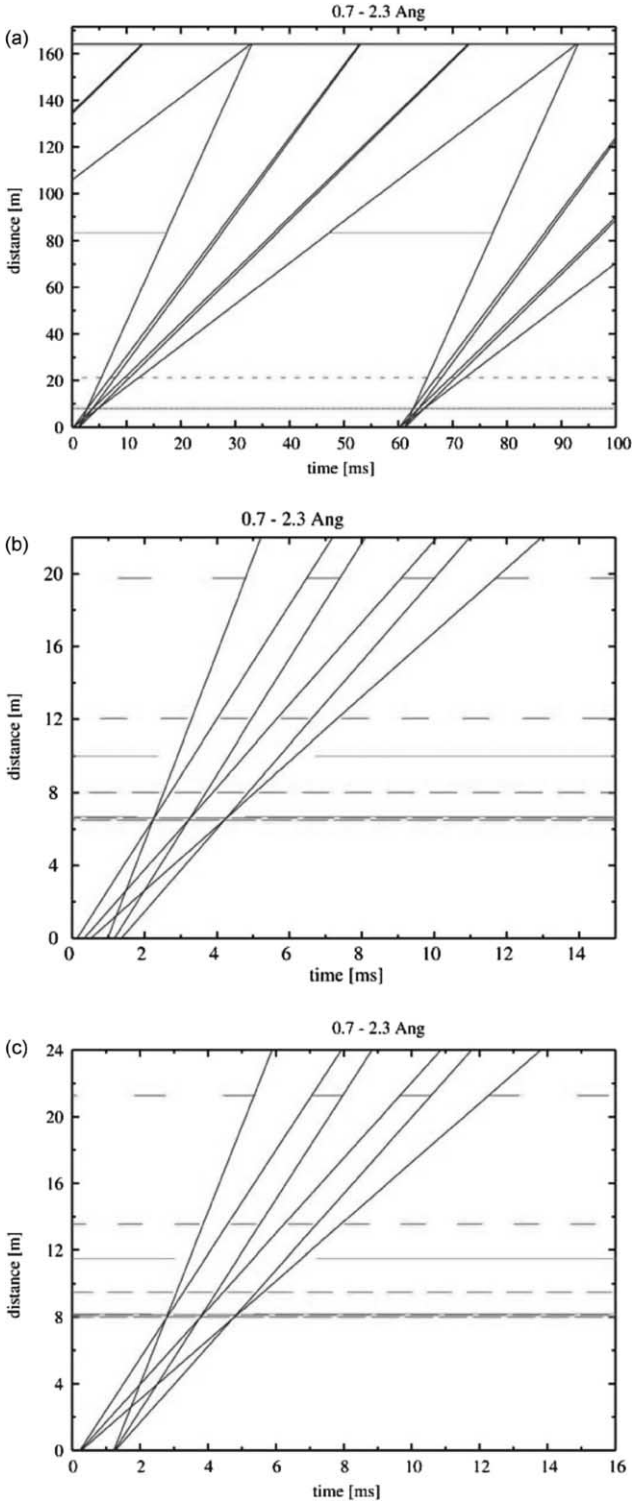

Figure 2. Distance-time-diagrams of the diffractometer installed on LPTS for wavelength band 0.7–2.3 Å: Frame definition choppers in the whole space and time range, 8 m set-up (a); all choppers within the first 24 m of the 6.5 m set-up (b) and the 8 m set-up (c), (space and time range are limited to illustrate pulse mirroring). In contrast to figure1 and distances given in the text, these are distances from the moderators.

SPTS (6.5 m), the pulse is assumed to be generated in a distance of $L_{\mathrm{src}} = 6.56\,\mathrm{m}$ from the source. For a pulse length $t_{\mathrm{p}} = 1\,\mathrm{ms}$, the bandwidth of such a single pulse is:

$$\Delta\lambda_{\mathrm{pulse}} = \frac{m_n}{h}\frac{t_{\mathrm{p}}}{L_{\mathrm{src}}} = 3.956\,\text{Å}\mathrm{m/ms}\cdot 1\mathrm{ms}/6.56\,m = 0.60\,\text{Å} \tag{2}$$

while the bandwidth that can be used in the instrument (with a total length $L_{\mathrm{tot}} = 156\,\mathrm{m}$ from the point of pulse generation to the detector and a pulse repetition time $T = 60\,\mathrm{ms}$) is

$$\Delta\lambda_{\mathrm{inst}} = \frac{m_n}{h}\frac{T}{L_{\mathrm{tot}}} = 3.956\,\text{Å}\mathrm{m/ms}\cdot 60\,\mathrm{ms}/156\,\mathrm{m} = 1.52\,\text{Å} \tag{3}$$

Therefore, three frames should be used via wavelength frame multiplication. This is realised by three choppers rotating with high frequency. A chopper 13.21 from the centre of the pulse shaping choppers defines these sub-frames (figure 2a). Additionally, two frame overlap choppers were positioned at 1.45 and 5.47 m from the pulse generating system. They shall prevent overlap between these three sub-frames (figure 2b). The frequency of these choppers depends on the distance from the pulse generating choppers (cf. figure 2b). The time T_{rep} between two generated pulses is usually identical with the length t_{p} of the long pulse, i.e. 1 ms. As it is planned that the three frames are neighbours at the detector, i.e. each frame covers $T_{\mathrm{frame}} = 20\,\mathrm{ms}$ of the 60 ms pulse repetition time. So the period of the rotation depends on the distance from the position of the pulse generation as

$$T_{1/3}(L) = (T_{\mathrm{frame}} - T_{\mathrm{rep}})\frac{L}{L_{\mathrm{tot}}} + T_{\mathrm{rep}} \tag{4}$$

The time t_{open} that the chopper has to be open to let the pulse pass is 20 ms at the detector and 0.025–0.24 ms (depending on the wavelength) at the pulse shaping choppers (figure 2). t_{open} is set to

$$t_{\mathrm{open}}(L) = T_{\mathrm{frame}}\frac{L}{L_{\mathrm{tot}}} \tag{5a}$$

for the frame definition chopper and

$$t_{\mathrm{open}}(L) = (T_{\mathrm{frame}} - t_{\mathrm{open}}(0)) \times \frac{L}{L_{\mathrm{tot}}} t_{\mathrm{open}}(0) = 19.76\,\mathrm{ms} \times L/156\,\mathrm{m} + 0.24\,\mathrm{ms} \tag{5b}$$

for the frame overlap choppers. All choppers have three openings as the first two choppers (to remain in the range of rotational frequency that is affordable nowadays.) So we get the frequency of rotation f and the angle α of each aperture:

$$f = \frac{1}{(3T_{1/3})} \tag{6}$$

$$\alpha = 120^{\circ}\frac{t_{\mathrm{open}}}{T_{1/3}} \tag{7}$$

But not every frequency can be used. The rate of opening of the chopper apertures must be a multiple of the repetition rate of the source. As a consequence, only certain distances can be used. The values used in the simulations are summarised in table 2. The time–distance-diagrams shown in figure 2 illustrate the system.

2.7 Ballistic guide

To decrease the losses inside the long guide, the principle of a ballistic guide is used, i.e. the guide widens to reduce the divergence and by this the number of reflections. The large cross-section is kept constant over the greater part of the guide, before a converging segment reduces the cross-section to its final value.

In this case, the ballistic guide starts after the third chopper; i.e. 12 cm downstream of the point of pulse generation. The cross-section is increased from 15×80 to $45 \times 130\,\mathrm{mm}^2$ (at 26.21 m). Between 124 and 139 m (from pulse generation) the guide is convergent to reach the cross-section of $20 \times 80\,\mathrm{mm}^2$ as used in the layout of the equivalent instrument at SPTS. Downstream of this point, the instruments are essentially identical.

3. MC simulations and data evaluation

We used the simulation package VITESS [11,12] to perform the simulations. About 1–3 billion trajectories (= random events) were started, of which typically 2,00,000 (SPTS) or 9000 (LPTS) reached the sample. Apart from various other reasons, this large difference is mainly caused by the fact that in the LPTS simulation all created neutrons are treated and the pulse generation takes place in the instrument. In contrast, the main part of the pulse generation of the SPTS instrument takes place already in the decoupled moderator, i.e. these neutrons do not have to be considered in these simulations.

The pulse shapes published in the ESS reference moderator characteristics [10] were used for the simulations (with the changes for the LPTS source discussed in chapter "source and extraction system"). The tails of the pulses were cut at 0.6 ms for the SPTS source and at 4 ms for the LPTS source. The effect of gravity was taken into account in all simulations. The extraction system was explicitly simulated using the module supermirror_ensemble.

Both instruments were simulated and the results compared. Since the instruments allow wavelength bands of only 1.6 Å, a few cases (0.7–2.3, 3.2–4.8 and 16–17.6 Å) were considered as examples for the whole wavelength range of interest (0.7–30 Å). The parameters of the simulations are summarised in tables 1 and 2.

Raw data were generated at two representative detector angles (175 and 45°) and the resulting intensity as a function of d-spacing compared. A cylindrical detector of 20 cm height ranging from 3.2 to 176.8° scattering angle with a grid of $1 \times 1\,\mathrm{cm}^2$ and 90% efficiency was assumed. The count rate at the detector was determined as a function of d-spacing.

Using a 180° chopper half way between source and detector causes a time interval in which the pulses overlap. This time cannot be used for data evaluation. So the time interval that can be used begins after the last (slow) neutrons of the previous pulse have arrived and ends before the first (fast) neutrons of the following pulse arrive. Furthermore, opening and closing of the frame definition chopper changes the signal. This so-called half-shadow state is also not used for data evaluation, thus the time interval used for data evaluation is further reduced. This concept was used for the frames and for the sub-frames.

The SPTS instrument was treated in the same way; the chopper in 12 m distance was regarded as the frame definition chopper determining the time interval for data evaluation.

4. Testing and improving the instrument layout

4.1 Feasibility of the frame multiplication concept

To show that the principle of frame multiplication works, we marked the trajectories at the second pulse-shaping chopper: It was noted which aperture of this chopper was passed.

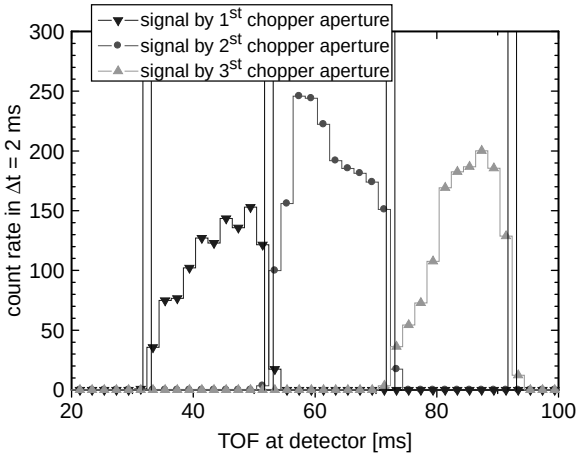

Figure 3. Three sub-frames generated via frame multiplication within one cycle of a long pulse source. Vertical bars indicate the time ranges that are not used for data evaluation due to overlap of the sub-frames. The sample was an incoherent scatterer.

Figure 3 shows that the sub-frames generated this way arrive one after the other within one period of the long pulse source. Only small overlap regions are found. They correspond to time intervals that are not used for data evaluation. Thus, frame overlap between sub-frames could be prevented effectively. So the whole achievable wavelength band can be used (cf. figure 2)—except for the small overlap ranges. For the short wavelength band, the ranges 0.802–1.255, 1.265–1.736 and 1.747–2.198 Å can be used (cf. figure 4). For comparison, the equivalent wavelength range for the SPTS is 0.835–2.062 Å.

The gaps in wavelength are significantly smaller than those in time, because the pulses are created at different times, separated by 1 ms. So only a time interval above 1 ms that is not used for data evaluation causes a gap in the usable wavelength band—here it is 1.407 ms.

The gaps in the usable wavelength range do not lead to gaps in the *d*-spacing coverage, since detectors cover different scattering angles. For highest resolution work one will only consider detectors above 164° which guarantees access to all *d*-spacing corresponding to the full wavelength band 0.802–2.198 Å.

4.2 Optimal extraction system

The first approach was to put the first pulse shaping chopper as close as possible to the moderator (6.5 m). This has the disadvantage that the three sub-frames reflect different parts of the pulse (cf. figure 2b). This is a result of the fact that three sub-frames are used, but the ratio of the bandwidths is $1.52/0.6 = 2.53$, not 3 (cf. equations (2) and (3)). As a consequence, the third sub-frame is partly created by the tail of the pulse. This results in a low intensity in its short wavelength (or TOF) part, which is visible in figure 3.

To overcome this problem, we have increased the distance between moderator and first pulse shaping chopper to 8.0 m. Figure 4 shows that indeed the distinct minimum at 1.85 Å can be clearly diminished, while the overall intensity remains roughly the same. (It should be added that it is probably favourable to adjust the instrument length, if it is not the aim to compare it with another instrument of particular features.) Unfortunately, there remains a lower intensity for the low-wavelength end of sub-frame one.

Another finding was that the intensity of longer wavelengths is decreased by the high inclination of mirror 1 of the extraction system (figure 1). Therefore, we have introduced a kink between mirror 2 and 3 (figure 1). The inclination of mirror 3 in front of the guide was

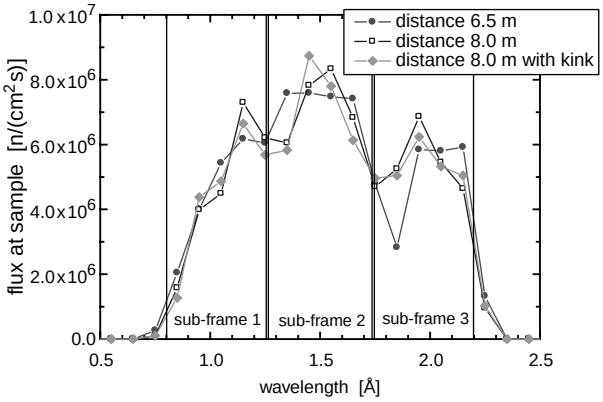

Figure 4. Count rate on sample for different extraction systems of the instrument on LPTS for wavelength band 0.7–2.3 Å. Vertical bars indicate the wavelength ranges that are used for data evaluation.

kept constant at 0.72°, because this defines the wavelength of switching over from the thermal to the cold moderator.

We could enhance the flux at the sample by about a factor of 2 in the range 3.2–4.8 Å—not shown here—by using such a kink in the extraction system (figure 1), while the count rate in the short wavelength range remained nearly the same (figure 4). This kink reduces the inclination of the outer mirror and thus the resulting divergence, while it keeps the large entrance width (4.8 cm) in front of the cold source and the optimal inclination of mirror 2 for the short wavelength neutrons from the thermal source (figure 1). The best design found so far has an outer mirror of 0.865° inclination. This set-up was used for the comparison with the instrument installed on the other target station.

5. Comparison of the instruments at different target stations

Figures 5–8 show the count rate at detector as a function of *d*-spacing (calculated from time-of-flight) for backscattering in different wavelength bands. Figure 9 shows it for forward scattering in the band 0.7–2.3 Å. As planned, the FWHM line widths are about the same for the two target stations.

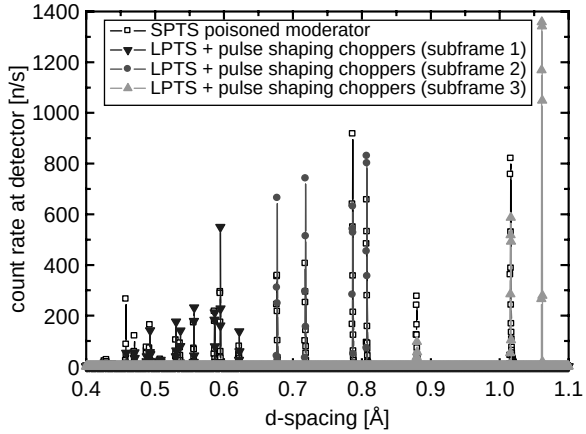

Figure 5. Backscattering (164–175°) powder spectra of Ni for a wavelength band of 0.7–2.3 Å obtained by diffractometers on SPTS (cold decoupled poisoned moderator) and LPTS (multi-spectral moderator, 1 ms option, pulse shaping choppers used).

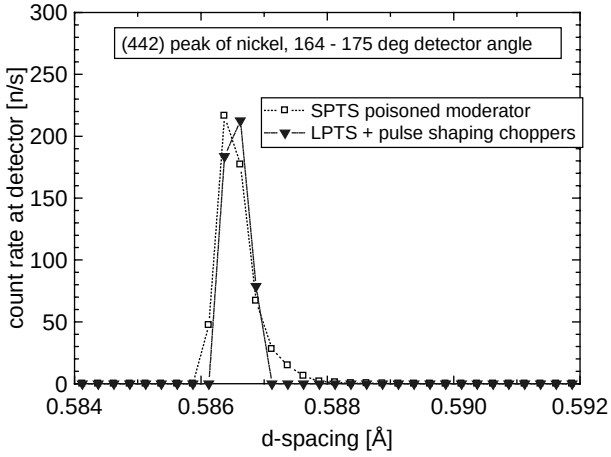

Figure 6. Comparison of peak intensity and shape between short and long pulse source of ESS for short wavelengths: the count rate at the detector is shown as a function of *d*-spacing for 164–175° detector angle.

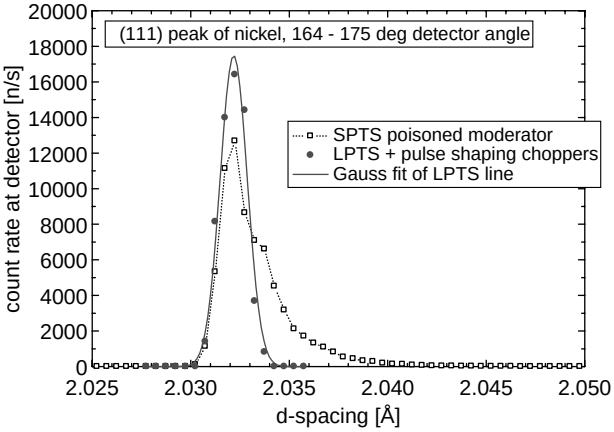

Figure 7. Comparison of peak intensity and shape between short and long pulse source of ESS for an intermediate wavelength range (3.2–4.8 Å): the count rate at detector is shown as a function of *d*-spacing.

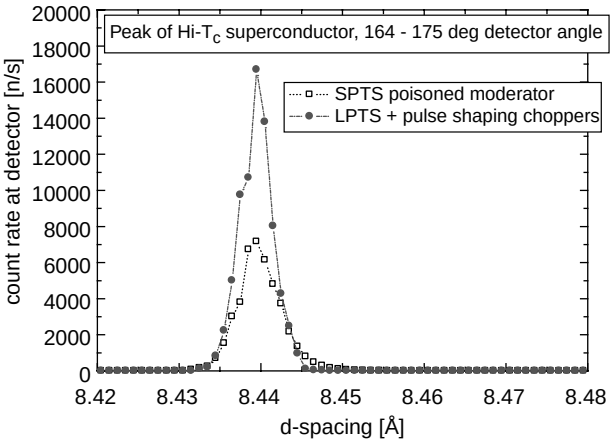

Figure 8. Comparison of peak intensity and shape between short and long pulse source of ESS for long wavelengths (range: 16.0–17.6 Å): the count rate at detector is shown as a function of *d*-spacing.

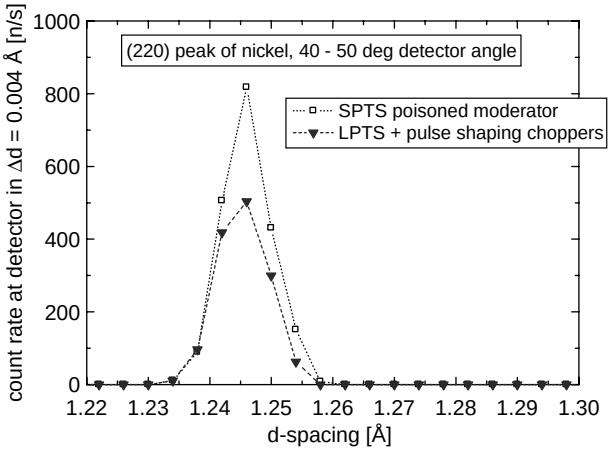

Figure 9. Comparison of peak intensity and shape between short and long pulse source of ESS for short wavelengths (0.7–2.3 Å, 1.2–1.5 Å for this line): the count rate at the detector is shown as a function of *d*-spacing for 40–50° detector angle.

Figure 5 shows the whole spectrum obtained by the wavelength band 0.7–2.3 Å in backscattering mode (164–175°). The (220) peak at 1.0613 Å is missing in the SPTS spectrum because of the restriction in time interval used for data evaluation. Due to overlap of subsequent pulses and half-shadow times, only the interval 10.981–27.103 ms can be used, which corresponds to a wavelength range of 0.835–2.062 Å or a *d*-spacing range of 0.418–1.041 Å (for detector coverage of 164–175°).

In this wavelength range, the peaks are of comparable height (see also figure 6). Apart from statistical effects, variations are due to the different parts of the long pulse that are mirrored to the detector by the pulse generating system (cf. figures 2–4). In the medium wavelength range (3.2–4.8 Å), the peak amplitude is higher for the LPTS compared to the SPTS by a factor of 1.4 (figure 7); in the long wavelength range (16–17.6 Å) by a factor of about 2.4 (figure 8)—if the high energy option and the improved coupled moderator are used.

In the backscattering regime the shape of the signal of the LPTS instrument is nearly symmetric; whereas the peaks of the SPTS instrument show a tail towards higher wavelengths (figures 6–8) caused by the tale of the pulse. The LPTS peaks can be fitted well by a Gaussian function (cf. figure 7). This allows a precise determination of the *d*-values, though the statistical accuracy is not high [13]. As an example, a fit of the (111) peak of nickel with the data shown in figure 7 yields $d = 2.03218$ Å (true value 2.03227 Å).

While the peaks of the LPTS instrument are centred on the true value, the peaks of the short pulse instrument are not. The reason is that the pulse starts at $t = 0$ and has its maximum at $\delta t > 0$; the time Δt belonging the peak maximum found at the detector depends on the pulse length itself and the resolution function of the instrument (including the chopper system) and is not generally known. So the peaks have to be empirically shifted to make it coincide with the true value. This is done in all diagrams shown here (figures 5–8). Because of this procedure, the *d*-values cannot be determined with the same precision on the SPTS.

If the asymmetric peak has a sharp edge, the separation of two neighbouring peaks (in the presence of noise) is facilitated [13]. But the steep edge of the SPTS peaks is not significantly steeper than both edges of the LPTS. Therefore, a better peak separation cannot be expected for the SPTS instrument.

For forward scattering, the peak created by the SPTS approaches a symmetric shape (figure 9), as the resolution is low and dominated by the spatial resolution and not by the time resolution of the pulse. A further consequence is the higher amplitude of this peak compared

to that by a LPTS. Neutrons belonging to the tail in backscattering contribute to the peak height here.

Both instruments can still be improved. Example for the SPTS are a higher coating of vertical walls of the straight guides (see above) or a shift of the frame definition chopper downstream to increase the time interval that can be used for data evaluation. For the LPTS-instrument, a reduction of the losses inside silicon or after the kink is possible. Also the ballistic guide might still be better adapted to small wavelengths. Additionally, using a wavelength dependent pulse centre would improve the results, especially for the short wavelength band.

The performance of such a powder diffractometer can be at least as good on a LPTS as it is on a SPTS, especially if it is used in backscattering mode to obtain high resolution. The LPTS instrument matches the performance of SPTS instrument in the case most favourable for SPTS: highest resolution offered by the poisoned moderator. The superior intensity for longer neutron wavelengths is important for larger elementary cells and weak magnetic order. Furthermore it is the more flexible instrument, because it is possible to increase the intensity by reducing the solution. Altogether the LPTS can be regarded as the better source for a diffractometer designed for measuring magnetic structures.

6. Summary

According to these MC simulations, the wavelength frame multiplication is feasible. A long pulse spallation source can be used very efficiently this way.

If both instruments have the same FWHM resolution and band width, the intensities are significantly higher above 2.5 Å and comparable down to 1 Å. The peak shape is always symmetric, centred on the true d-value and allows a more precise determination of d-spacings (with a simple Gaussian function). On the other hand, the separation of peaks might be worse compared to the instrument on the SPTS. Another advantage of the concept to use a long pulse spallation source plus pulse shaping choppers (instead of a short pulse spallation source) is that the pulse length can be adjusted. So the required resolution (for the sample under investigation) can be set, i.e. one is free to choose wavelength and resolution. In contrast, using the SPTS there is only one resolution for each wavelength.

Acknowledgement

We like to thank Sergey Manoshin for his suggestions to improve the ballistic guide. This work has been supported by the SCANS network within the “Improving human potential programme” of the European Commission under contract HPRI-CT-1999-500013.

References

[1] G. Zsigmond, K. Lieutenant and F. Mezei, Monte Carlo simulations of single-crystal spectroscopy and diffraction at spallation sources, Appl. Phys. A **74**([suppl.]), S224 (2002).
[2] G.S. Bauer, M. Butzek, H. Conrad, D. Filges, F. Goldenbaum, P. Jung, G. Mank and R. Moormann, Target station and technical layout, in *The ESS Project Vol III, Technical Report* (ESS Council, Jülich, Germany, 2002), chapter 4.2.
[3] M. Russina and F. Mezei, Multiplexing chopper systems for pulsed neutron source instruments, Proc. SPIE (Int. Soc. f. Opt. Eng.) **4785** 24 (2002).
[4] K. Lieutenant, G. Zsigmond, S. Manoshin, M. Fromme, H.N. Bordallo, J.D.M. Champion, J. Peters and F. Mezei, Neutron instrument simulation and optimization using the software package VITESS, Proc. SPIE (Int. Soc. f. Opt. Eng.) **5536** 134 (2004).
[5] Instrumentation Task Group of the ESS, *The ESS Project Vol. IV, Instruments and User Support* (ESS Council, Jülich, Germany, 2002), pp. 2–22.

[6] F. Mezei, Instrumentation concepts: Advances by innovation and building on experience, in *The ESS Project Vol II, New Science and Technology for the 21st Century* (ESS Council, Jülich, Germany, 2002), chapter 3.
[7] F. Mezei and M. Russina, Patent application of 23.01.2002, No. 10203591.1 (Germany).
[8] F. Mezei and M. Russina, Neutron beam extraction and delivery at spallation neutron sources, Physica. B **283** 318 (2000).
[9] F. Mezei, Comparison of neutron efficiency of reactor and pulsed source instruments. in *Proc. ICANS-XII* Rutherford Appleton Laboratories, UK, RAL report No. 94 1993, pp. 1–377
[10] F. Mezei, 2000, ESS reference moderator characteristics for generic instrument performance evaluation, <http://www.hmi.de/bereiche/SF/ess/ESS-moderators.pdf; Picture gallery for the ESS reference moderators version 4.12.00, http://www.hmi.de/bereiche/SF/ess/ESS_mod_pics.pdf>
[11] <http://www.hmi.de/projects/ess/vitess>
[12] G. Zsigmond, K. Lieutenant and F. Mezei, Monte Carlo simulations of neutron scattering instruments by VITESS—Virtual instrumentation tool for ESS, Neutron News **13**(4) 11 (2002).
Q1 [13] D.S. Sivia, *Data Analysis: A Bayesian Tutorial*, (1996), p. ?.